Amplitude modes in cis-$(CH)_x$: second-order resonance Raman scattering

J. Phys.: Condens. Matter **2** (1990) 239–244. Printed in the UK

LETTER TO THE EDITOR

Amplitude modes in *cis*-$(CH)_x$: second-order resonance Raman scattering

F Coter†, E Ehrenfreund† and B Horovitz‡

† Physics Department and Solid State Institute, Technion—Israel Institute of Technology, Haifa, Israel

‡ Physics Department, Ben-Gurion University, Beersheba, Israel

Received 19 October 1989

Abstract. The amplitude mode formalism is used to account simultaneously for the first- and second-order resonance Raman scattering in *cis*-$(CH)_x$. The Raman cross-section is calculated assuming one-dimensional semiconducting band structure with finite electronic lifetimes. The strong overtone structure is the sharply peaked dynamic conductivity and its derivatives. Contrary to previous suggestions, no gap states are needed to explain the strong multiphonon Raman cross-section.

The Raman active vibrational A_g modes in *trans*-$(CH)_x$ were shown to be coupled to the π-electrons and to be described as amplitude modes of the dimerisation gap [1, 2] which is associated with the bond alternation pattern. The intermode couplings and their relations to the gap could be verified using the unique dispersion property of the resonant Raman scattering (RRS) spectrum of *trans*-$(CH)_x$. As the laser excitation energy, ω_L, is increased the first-order RRS frequencies of the three A_g modes shift upward and their relative intensities change [3]. This feature provides unique interrelation between the vibrational modes, which is fully accounted for by the amplitude modes model [1, 2, 4].

The amplitude mode model was also applied to non-degenerate ground state systems where the electronic gap has an extrinsic contribution [5]. In systems such as polythiophene [6, 7], the unique relation between the Raman active A_g modes and the doping-induced, or photoinduced, infrared active vibrations (IRAV) provides the evidence for the existence of amplitude modes. In the case of the non-degenerate ground state system *cis*-$(CH)_x$ [8, 9], the parameters are less contained in view of the absence of IRAV modes and the lack of dispersion.

Multiphonon RRS of *cis*-$(CH)_x$ and *cis*-$(CD)_x$ were reported by several groups [10, 11]. Unlike in the case for *trans*-$(CH)_x$, strong second- and higher-order RRS lines were observed. This strong series of overtones was taken as an indication for strong lattice relaxation due to localised intragap defects [9, 11].

In this letter we show that the multiphonon overtones may be fully accounted for by the amplitude mode formalism for a Peierls-like model. There is no need for localised intragap defects to explain the strong overtones. We show that for a strictly one-dimensional (1D) system the overtones are infinitely strong; finite overtone intensity can result from finite electronic lifetime effects.

0953-8984/90/010239 + 06 $03.50

In this section, we evaluate the Raman cross-section for the Peierls model. We derive the results in the adiabatic limit, $\omega \ll \omega_L$, by taking the derivatives of the frequency dependent electronic conductivity, $\sigma(\omega)$ [12].

The amplitude modes yield a time dependent modulation of the gap of the form $\Delta + \delta(t)$, $\delta(t) \ll \Delta$. Since this time variation is slow (the adiabatic limit) one may consider the electronic conductivity of frequency ω_L to be time dependent with the form $\sigma(\omega_L, \Delta + \delta(t))$:

$$\sigma(\omega_L, \Delta + \delta(t)) = \sigma(\omega_L, \Delta) + (\partial\sigma/\partial\Delta)\delta(t) + \tfrac{1}{2}(\partial^2\sigma/\partial\Delta^2)\delta^2(t) + \ldots. \tag{1}$$

The nth term of this series represents the n-phonon Raman scattering with the cross-section proportional to $|\partial^n\sigma/\partial\Delta^n|^2$.

The cross-section for the first-order Raman process was derived previously [13]:

$$\sigma^{(1)} = -(\omega_L^2/c^4)\sin^2\theta|\partial\sigma/\partial\Delta|^2 \operatorname{Im} D(\omega) \tag{2}$$

where θ is the angle between the chain direction and the light polarisation and $D(\omega)$ is the dressed phonon propagator

$$D(\omega) = 2\lambda D_0(\omega)/N(0)[1 + (1 - 2\tilde{\lambda})D_0(\omega)]. \tag{3}$$

In equation (3) $N(0)$ is the density of states at the Fermi level and $D_0(\omega)$ is given by

$$D_0(\omega) = \sum_n \frac{\lambda_n}{\lambda} \frac{\omega_n^{02}}{\omega^2 - \omega_n^{02} - i\omega\gamma_n} \tag{4}$$

where ω_n^0 are the bare mode frequencies, γ_n is the natural phonon width and λ_n is the dimensionless electron–phonon coupling constant for the nth mode, with $\lambda = \Sigma\lambda_n$. As can be seen from equations (2) and (3), the first-order RRS frequencies are the solutions of

$$\mathrm{Re}D_0(\omega) = -1/(1 - 2\tilde{\lambda}) \tag{5}$$

where $2\tilde{\lambda}$ is the renormalised force constant due to the π-electrons [1, 4].

The expansion (1) assumes just the adiabatic condition, while electron–electron interactions are included in $\sigma(\omega)$. To obtain a tractable expression for the resonance effect ($\propto \partial\sigma(\omega_L, \Delta)/\partial\Delta$) we assume the Peierls model (not electron–electron interactions) for which $\sigma(\omega) = \sigma_0(\omega)$ [14]

$$\sigma_0(\omega) = (\omega_p^2/4\pi i\omega)(g(\omega, \Delta) - 1) \tag{6}$$

where $\omega_p = (4\pi e^2 v_F^2 N(0))^{1/2}$ is the plasma frequency. For linear dispersion $\varepsilon = \hbar v_F k$, the function g is given by [13]

$$g(\omega, \Delta) = \int_{-E_c}^{E_c} \frac{2\Delta^2}{E[4E^2 - (\omega + i\Gamma)^2]}\,d\varepsilon \tag{7}$$

where $E = (\varepsilon^2 + \Delta^2)^{1/2}$, 2Δ is the gap, v_F the Fermi velocity and $E_c = \hbar v_F k_F$ is the cut-off energy ($\simeq$ the bandwidth). For infinitely long electronic lifetime, $\Gamma \to 0$ and the nth derivative $\partial^n\sigma_0/\partial\Delta^n$ diverges at $\omega_L \simeq 2\Delta$, thus predicting infinitely strong multiphonon RRS. In real systems, however, the RRS intensity is finite due to either finite Γ or 3D effects such as interchain coupling. In previous treatments [2, 4] of first-order RRS, 3D effects were taken into account by arbitrarily cutting off the function $|\partial\sigma_0/\partial\Delta|^2$ near $\omega_L/2\Delta = 1$ to allow for finite cross-section. This procedure does not, however, yield higher-order

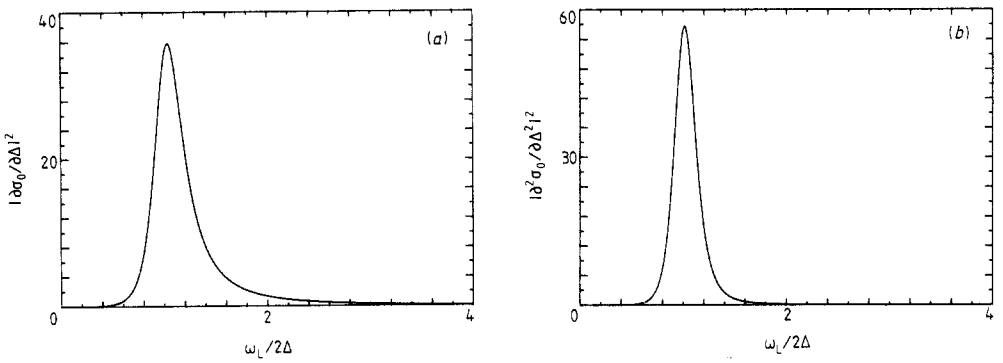

Figure 1. The functions (*a*) $|\partial\sigma_0/\partial\Delta|^2$ and (*b*) $|\partial^2\sigma_0/\partial\Delta^2|^2$ versus $\omega_L/2\Delta$ for $\Gamma/2\Delta = 0.2$.

RRS since higher-order derivatives are grossly distorted. Here, instead, we take into account the effect of finite lifetime in the Peierls model by allowing $\Gamma > 0$ in equation (7). When this is done the integral (7) and its derivatives are finite at $\omega_L \simeq 2\Delta$ and may be directly calculated. The function g is then given by

$$g(\omega_L, \Delta) = [1/2B(1 + A)]\{\ln[i(x_0 - B)] - \ln[i(x_0 + B)]\} \tag{8}$$

where $A = (\omega_L/2\Delta)^2 - (\Gamma/2\Delta)^2 - 1 + i\omega_L\Gamma/2\Delta^2$, $B = [A/(A + 1)]^{1/2}$ $(\mathrm{Im}B > 0)$, $x_0 = \sin(\tan^{-1}(E_c/\Delta)) \simeq 1$ and $\ln z = \ln|z| + i \arg z$ $(-\pi/2 < \arg z < \pi/2)$ is the complex logarithm. Using these results, we have calculated the function σ_0 and its derivatives. The function $|\partial\sigma_0/\partial\Delta|^2$ is plotted in figure 1(*a*) for $\Gamma/2 = 0.2$. Note that $|\partial\sigma_0/\partial\Delta|^2$ does not diverge, as is the case for $\Gamma = 0$ [13], but has instead a strong peak near resonance at $\omega_L \simeq 2\Delta$.

The cross-section for the second-order Raman scattering corresponds to the diagram in figure 2 . More generally, it can be derived from the current $j^{(2)}$ due to an electric field E_0 and the last term in equation (1)

$$j^{(2)}(\omega) = \frac{1}{2}\frac{\partial^2\sigma}{\partial\Delta^2} E_0 \int \delta^2(t) e^{-i\omega t}\, dt. \tag{9}$$

We expand $\delta(t) = \Sigma_m a_m \delta_m \exp(i\omega_m t)$ in the normal modes δ_m of the interacting system with eigenfrequencies ω_m and use (δ_D is the Dirac delta function)

$$\mathrm{Im}\, D(\omega) = \pi \sum_m |a_m \delta_m|^2\, \delta_D(\omega_m - \omega). \tag{10}$$

The radiated power ($\propto |j(\omega)|^2$) then yields the cross-section

$$\sigma^{(2)} = \frac{\omega_L^2}{2\pi c^4} \sin^2\theta \left|\frac{\partial^2\sigma}{\partial\Delta^2}\right|^2 \int_{-\infty}^{\infty} \mathrm{Im}\, D(\omega')\, \mathrm{Im}\, D(\omega - \omega')\, d\omega'. \tag{11}$$

Figure 2 corresponds to the Peierls model with $\sigma(\omega) = \sigma_0(\omega)$.

Equation (11) contain two main factors. The first is a phononic convolution of Im $D(\omega')$ and Im $D(\omega - \omega')$ [15]. It gives rise to strong peaks at all frequencies ω which are, as expected, the sums of two first-order Raman frequencies. The second factor is $|\partial^2\sigma/\partial\Delta^2|^2$ which determines the resonance enhancement of the second-order cross-section. The function $|\partial^2\sigma_0/\partial\Delta^2|^2$, the resonance enhancement for the Peierls model, is shown in figure 1(*b*), again showing a strong peak near $\omega_L = 2\Delta$.

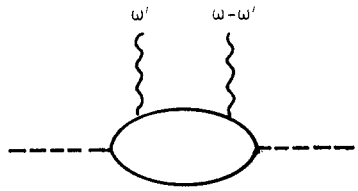

Figure 2. The second-order Raman amplitude for the Peierls model.

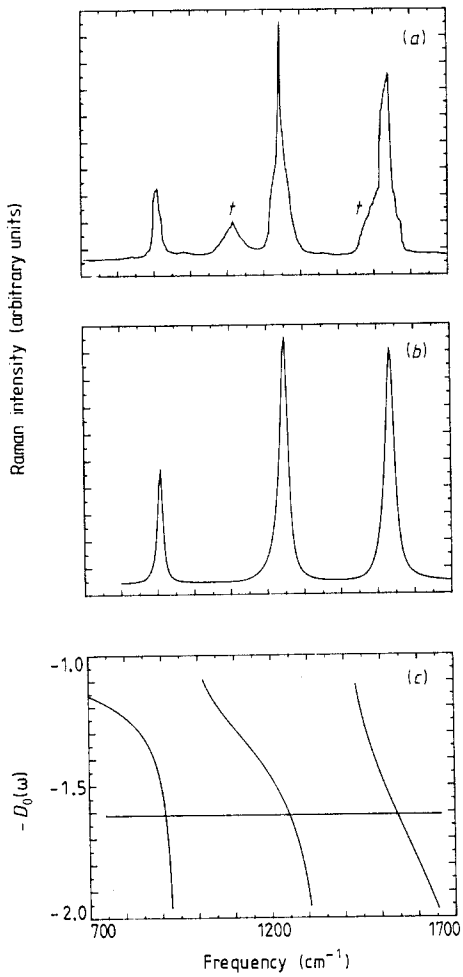

Figure 3. First-order RRS in *cis*-$(CH)_x$: (*a*) measured [10]; (*b*) calculated; and (*c*) the function $D_0(\omega)$. *t* indicates the RRS of *trans*-$(CH)_x$ present in the *cis*-$(CH)_x$ samples. The horizontal line in (*c*) gives the value of $-(1-2\tilde{\lambda})^{-1}$ appropriate for *cis*-$(CH)_x$; its intersections with the three branches of $D_0(\omega)$ give the RRS frequencies. The slopes at the intersections are inversely proportional to the relative intensities.

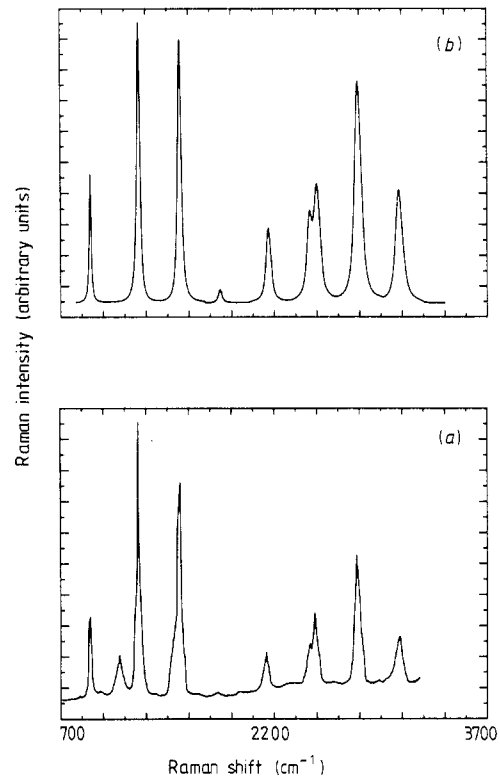

Figure 4. First- and second-order RRS spectra: (*a*) measured [10], and (*b*) calculated for $\Gamma/2\Delta = 0.2$.

Table 1. A comparison between relative intensities of first- and second-order RRS in *cis*-$(CH)_x$. The experimental values were taken from [10]. The fundamental line frequencies are: $\omega_1 = 910\,cm^{-1}$, $\omega_2 = 1250\,cm^{-1}$ and $\omega_3 = 1540\,cm^{-1}$. $2\omega_2$ and $\omega_1 + \omega_3$ are not well resolved, so the sum of their intensities is given in the table. For the overall intensity agreement between first and second order see figure 4.

	First order			Second order				
	ω_1	ω_2	ω_3	$2\omega_1$	$\omega_1+\omega_2$	$\omega_1+\omega_3$ and $2\omega_2$	$\omega_2+\omega_3$	$2\omega_3$
Experiment	0.18	0.66	1.00	0.070	0.55	1.72	1.72	1.00
Calculation	0.27	0.96	1.00	0.064	0.45	1.35	1.84	1.00

The ratio, R_{12}, of the strength of the second- to first-order RRS is dominated mainly by Γ. For $\Gamma \to 0$, R_{12} diverges and multiphonon processes are stronger than the first-order process. For finite Γ the efficiency of the second-order scattering decreases roughly as $R_{12} \simeq \Gamma^{-\alpha}$ with $\alpha \simeq 2$. Second-order RRS yields, thus, an indication about the parameter Γ in the damped Peierls model.

A typical first-order RRS spectrum of *cis*-$(CH)_x$ is shown in figure 3. As in the *trans* isomer, it is characterised by three resonantly enhanced lines. But unlike *trans*-$(CH)_x$, here the lines are sharp and do not shift with the laser wavelength. The intensities of these lines are affected by the strong luminescence (centred at $\simeq 1.9$ eV) and the vibronic structure on the absorption curve. Since our amplitude mode analysis does not take these effects into account, we have chosen a spectrum where these effects are minimal. In this way we were able to find a function $D_0(\omega)$ that can fit simultaneously the frequencies and the relative intensities of the first-order RRS at an excitation wavelength $\lambda_L = 4880$ Å, where there is no observed luminescence. $D_0(\omega)$ is shown in figure 3 together with the calculated spectrum based on equation (2). The overall agreement with the measured spectra is very good.

Starting from the above $D_0(\omega)$, we have calculated the second-order spectrum using equation (10) with Γ as the single free parameter. Figure 4 shows the result of the calculation for $\Gamma/2\Delta = 0.2$, while table 1 gives the relative intensities of the various lines. As can be seen, the fit gives very good agreement for the second-order frequencies and relative intensities.

Note, however, that the ratio between the strengths of the second- to first-order RRS (R_{12}) is very sensitive to the state of isomerisation of *cis*-$(CH)_x$. Samples of *cis*-$(CH)_x$ are never 100% *cis*, and R_{12} strongly decreases with the *trans* content, and with the amount of defects. Therefore, the value $\Gamma/2\Delta = 0.2$ found above is probably an overestimate in which the effect of interchain coupling interactions is also contained. The value of $\Gamma/2\Delta$ for completely isomerised *cis*-$(CH)_x$ may be considerably smaller than 0.2.

In conclusion, the strong second-order (and presumably higher-order) RRS in conjugated polymers can be explained simply by their 1D nature. The strength of the second-order spectrum can be related to the finite electronic lifetime, $\hbar/\Gamma$. Good results are obtained for *cis*-$(CH)_x$, without involving any intragap defect states needed in previous treatments [9, 11] to account for the strong overtone structure.

This work was supported by the US–Israel Binational Science Foundation (BSF), Jerusalem, Israel.

References

[1] Horovitz B 1982 *Solid State Commun.* **41** 729
[2] Vardeny Z, Ehrenfreund E, Brafman O and Horovitz B 1983 *Phys. Rev. Lett.* **51** 2326
[3] Harada I, Furukawa Y, Tasumi M, Shirakawa H and Ikeda S 1980 *J. Chem. Phys.* **73** 4746
Lichtmann L S, Sarhangi A and Fitchen D B 1980 *Solid State Commun.* **36** 896
Kuzmany H 1980 *Phys. Status Solidi* b **97** 521
Lefrant S 1983 *J. Physique Coll.* **44** C3 247
[4] Ehrenfreund E, Vardeny Z, Brafman O and Horovitz B 1987 *Phys. Rev.* B **36** 1535
[5] Brazovskii S and Kirova N 1981 *JETP Lett.* **33** 4
[6] Vardeny Z, Ehrenfreund E, Brafman O, Heeger A J and Wudl F 1987 *Synth. Met.* **18** 183
[7] Poplawski J, Ehrenfreund E, Glenis S and Frank A J 1989 *Synth. Met.* **28** 335
[8] Ehrenfreund E, Vardeny Z, Brafman O and Horovitz B 1985 *Mol. Cryst. Liq. Cryst.* **117** 367
[9] Youjiang G and Lu Y 1986 *Solid State Commun.* **58** 407
For their calculations of $D_{\parallel}(\omega)$ for *cis*-$(CH)_x$, these authors used the IRAV lines of *trans*-$(CH)_x$ as an approximation
[10] Lichtmann L S, Imhoff E A, Sarhangi A and Fitchen D B 1984 *J. Chem. Phys.* **81** 168
[11] Siebrand W and Zgierski M Z 1984 *J. Chem. Phys.* **81** 185
[12] Chantry G W 1971 *The Raman Effect* ed A Anderson (New York: Dekker) p 49
[13] Horovitz B, Vardeny Z, Ehrenfreund E and Brafman O 1986 *J. Phys. C: Solid State Phys.* **19** 7291
[14] Lee P A, Rice T M and Anderson P W 1974 *Solid State Commun.* **14** 703
[15] A similar convolution formula was derived by
Schmeltzer D, Ohana I and Yacoby Y 1986 *J. Phys. C: Solid State Phys.* **19** 2113